We are IntechOpen,
the world's leading publisher of
Open Access books
Built by scientists, for scientists

6,900
Open access books available

186,000
International authors and editors

200M
Downloads

Our authors are among the

154
Countries delivered to

TOP 1%
most cited scientists

12.2%
Contributors from top 500 universities

CLARIVATE ANALYTICS
BOOK CITATION INDEX
INDEXED

WEB OF SCIENCE™

Selection of our books indexed in the Book Citation Index
in Web of Science™ Core Collection (BKCI)

Interested in publishing with us?
Contact book.department@intechopen.com

Numbers displayed above are based on latest data collected.
For more information visit www.intechopen.com

Gas Hydrate Formation Kinetics in Semi-Batch Flow Reactor Equipped with Static Mixer

Hideo Tajima
Niigata University
Japan

1. Introduction

Gas hydrate is an ice-like solid and a kind of inclusion compounds of which the cage-like structure formed by hydrogen-bonded water molecules can include various kinds of guest gas molecules. In general, gas hydrates are formed with "host" water and "guest" gas molecules under lower temperature and higher pressure conditions, but sometimes large differences in the hydrate formation conditions are observed among guest gases. In such cases, if gas hydrate is formed with such a gaseous mixture, it can be anticipated that the component of which the hydrate formation condition is milder (that is, higher temperature and lower pressure conditions relatively) could be enriched in the hydrate phase. Effective gas separation, or higher selectivity, can be achieved for gas mixtures with larger differences in the hydrate formation conditions. On the other hand, multi-component gas hydrates are formed under higher pressure and lower temperature conditions in which any component of gaseous mixture can change to hydrate.

Several applications have been proposed in environmental and energy fields by using the inclusion abilities in the framework of gas hydrates; natural gas transport (Gudmundsson & Børrehaug, 1996), gas storage (Lee et al., 2005), and gas separation (Kang & Lee, 2000) and so on, and thus many investigations for gas hydrate formation, especially thermodynamics and gas hydrate formation kinetics, have been carried out in batch systems. The solid hydrate can be dissociated to recover a product gas. The selectivity and production rate are key factors in determining the performance of hydrate-based applications. Although the selectivity is limited by the thermodynamic equilibrium of the hydrate phase and the feed vapour phase (Nagata et al., 2009), the production rate is dependant on the hydrate formation rate and the system design.

Gas hydrate-based applications would require an efficient formation or production process of gas hydrates, and the elucidation of the formation mechanism of gas hydrates. Gas hydrate formation is similar to crystallization from liquid mixture, and gas-liquid system changes to liquid-solid or gas-solid systems. In general, it is known gas hydrate forms on gas-liquid interface, and thus the gas-liquid interfacial area, the driving force, and kinetic constant can affect hydrate formation. Therefore, an efficient way to increase these factors is necessary for continuously forming gas hydrate solid in gas-liquid system. For example, several efficient processes to increase the interfacial area for gas hydrate formation have been demonstrated, including a spray (Fukumoto et al., 2001) or jet reactor (Szymcek et al., 2008; Warzinski et al., 2008), and a bubble column (Luo et al, 2007; Hashemi et al., 2009)

besides general stirred tank. However, gas hydrate formation is very complicated by the presence of three phases (gas-liquid-solid) during gas hydrate formation; the formation of solid (gas hydrate) can occur on gas-liquid (water) interface.

Although many investigations about gas hydrate formation have been published, this chapter deals with gas hydrate formation kinetics with focusing on author's research with a semi-batch flow reactor equipped with static mixer. In the broad sense, this chapter will cover the multiple flow and pipe flow. The gas hydrate formation is composed of two main processes as well as crystallization; hydrate nucleation and hydrate growth processes. This chapter focuses attention on the overall gas hydrate formation process, and thus discusses the hydrate formation process based on the experimental data by varying thermodynamic, mechanical, and chemical conditions.

2. Semi-batch flow reactor with static mixer

In author's study, gas hydrate formation from gas-liquid fluids is carried out in Kenics static mixer. Static mixers are motionless mixing devices with fixed "mixing elements" arranged in a straight pipe. The Kenics static mixer experiments demonstrated that two fluids (drop/bubble and water) are efficiently agitated with the mixing elements and are subsequently converted to hydrate formed on the drop/bubble surface at specific temperature and pressure conditions (Tajima et al., 2004, 2007). Several structures of mixing element are designed for efficient agitation/mixing of fluids more than one. Compared with stirred tank type mixers, static mixers also generally provide continuous operational availability, small size and space requirements, flexibility in the process installation, and low power requirements (Godfrey, 1997).

Fig.1 shows the author's semi-batch flow reactor with static mixer for continuous gas hydrate formation system. Kenics-type mixing elements of a stainless steel static mixer are used. There are 24 mixing elements and these are inserted into a pyrex glass tube (455 mm, i.d. 11.0 mm) for low pressure conditions (< 0.5 MPa) or into a stainless steel tube (same size to glass tube) with a pyrex glass window for high pressure conditions (< 2.0 MPa). Static mixer can achieve the mixing performance depending on the gas and water flow rates. The target gas is injected with mass flow controller at the bottom of the reactor and the water flow rate is operated with the water supply pump either counter or co-current to the gas flow direction. At water flow rate of zero this system is regarded as a semi-batch system that only the gas go in and out of the reactor. The injected gas is converted to gas hydrate in the static mixer unit and unconverted gas is vented from at the top of the reactor. Transport of formed hydrate particles are carried out with the water fluid, and the hydrate particles are settled and separated at the recovery vessel. Water without large hydrate particle, therefore, is always supplied to the reactor. The recovery vessel is set up in a manner to prevent the gas hydrate blocking the gas supply nozzle or the reactor, and thus the continuous hydrate formation is achieved. Pressure and temperature conditions for target gas hydrate formation are selected according to gas-water-hydrate equilibrium condition in available literature data. The reactor, the recovery vessel, and the water supply pump are all placed in a low temperature thermostatic chamber to control the system temperature. Experimental pressure is controlled within ±0.01 MPa by a pressure-regulating valve installed on the downstream side of the reactor. Various gas hydrate formations are carried out under constant pressure and temperature conditions.

To calculate the hydrate formation rate, outlet gas flow rates are measured by a mass flow meter after the gas had passed through the reactor. Gas hydrate formation was confirmed by both visual observations and variations in outlet gas flow rates. The gas uptake rate into hydrate was determined using the difference between inlet and outlet gas flow rates, assuming that all the gas molecules are used to form hydrate. The gas uptake rate is equal to overall gas hydrate formation rate (r_{hy}).
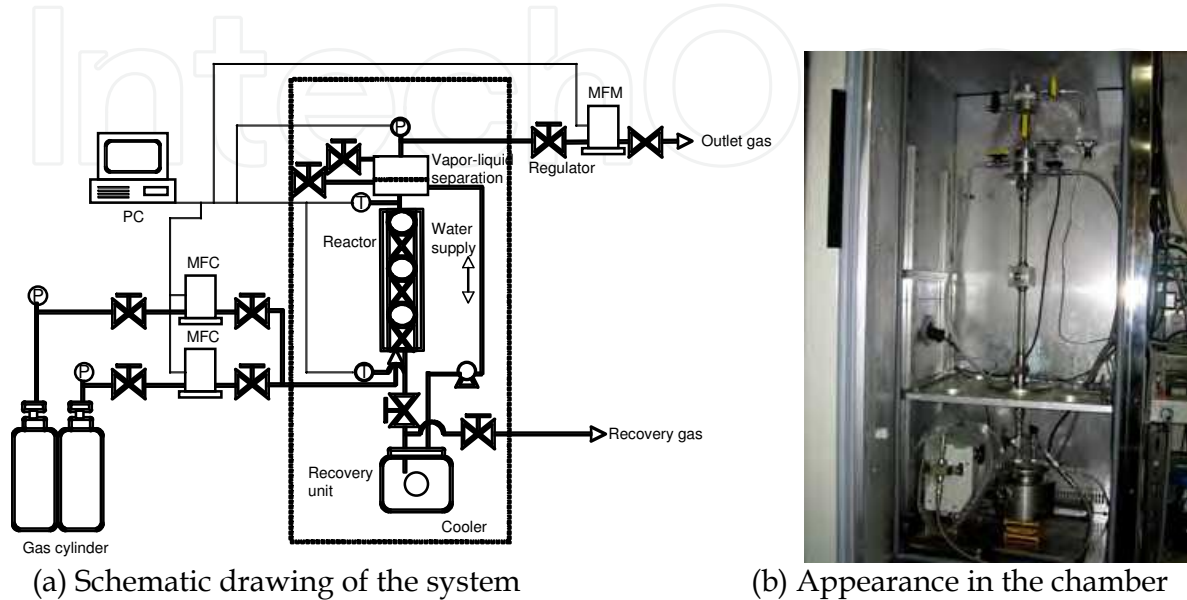

(a) Schematic drawing of the system   (b) Appearance in the chamber

Fig. 1. Semi-batch flow reactor with static mixer for gas hydrate formation system

Elapsed time ⟶   Elapsed time ⟶

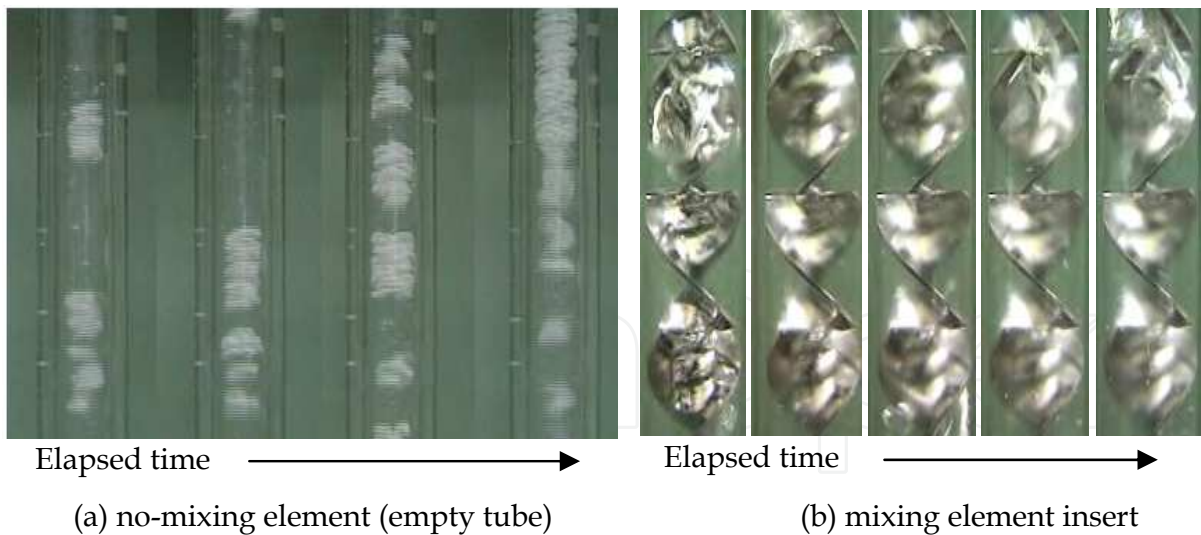(a) no-mixing element (empty tube)   (b) mixing element insert

Fig. 2. Static mixing effect on gas-water-hydrate fluids (CH_2FCF_3 gas-water system at 276K and 0.20 MPa with 200 mL/min of gas flow rate)

Fig.2 shows the static mixing effect on gas hydrate formation from CH_2FCF_3 gas-water system. When the gas hydrate formation is carried out in empty tube, bubble surface is covered with hydrate, and consequently the flow channel in the tube is blocked (Fig.2a). The insert of mixing elements can form hydrate slurry and prevent the tube blockage by mixing functions long time (Fig.2b). This result indicates that the mixing function of this mixing

element is important for the removal of hydrate film from bubble surface. The details of mixing function effect have been mentioned in previous literature for liquid CO_2-water system in the co-current flow reactor (Tajima et al., 2005). In the semi-batch flow reactor, the hydrate slurry formation is depending on not only mixing functions of the mixing elements but other conditions; operation pressure, operation temperature, gas and water flow rates, gas species, and so on. The relation between the hydrate formation pattern and these conditions will be discussed again later.

3. Hydrate formation rate analysis

There are many discussion about gas hydrate formation kinetics. With regard as this point, another book about natural gas hydrate is available (Sloan and Koh, 2008). Although gas hydrate nucleation and growth processes have been investigated and discussed by many researchers, temperature difference, chemical potential difference, and fugacity difference are selected as the driving force. Here, let's say overall gas hydrate formation rate r_{hy} is expressed by the chemical potential difference between formation and equilibrium as the driving force (Englezos et al., 1987; Daimaru et al., 2007; Li et al., 2009; Tajima et al., 2010a).

$$r_{hy} = -\frac{dn}{dt} = aK^* \left(\mu_g - \mu_{eq} \right) \tag{1}$$

where n is the number of moles of target gas (guest gas) consumed in the gas phase, t is elapsed time, aK^* is the hydrate formation rate constant, a is the interfacial area, K^* is the overall kinetics constant, and μ_g and μ_{eq} are chemical potentials of guest gases in the gas phase and hydrate phase, respectively. The overall kinetics constant K^* will be expressed using the mass transfer coefficient k_L and the hydrate crystal growth constant k_f.

$$\frac{1}{K^*} = \frac{1}{k_L} + \frac{1}{k_f} \tag{2}$$

This idea is very similar to the treatment of crystal growth behavior of crystalization (the nucleation process is ignored because of crystal seed addition) and gas absorption with reaction in chemical engineering field.

$$r_{hy} = -\frac{dn}{dt} = aK^* \cdot RT\ln\left(\frac{f_g}{f_{eq}} \right) \tag{3}$$

Although Eq.(2) may have to take account of the hydrate nucleation actually, we omits the part of the nucleation here. Because the chemical potential terms can be reduced to the fugacity of the gas, Eq.(1) can be easily transformed to the form of Eq.(3). R is the gas constant, T is the operation temperature, and f_g and f_{eq} are the fugacities of the guest molecules in vapour phase and in hydrate phase, respectively. The fugacity f_{eq} is equal to that under equilibrium. Because the fugacity can be simply expressed by the pressure and fugacity coefficient ϕ (Eq.(4)), Eq.(3) will be appropriated by Eq.(5).

$$f = \phi \cdot P \tag{4}$$

$$r_{hy} = -\frac{\mathrm{d}n}{\mathrm{d}t} \approx aK^* \cdot RT \ln\left(\frac{P_g}{P_{eq}}\right) \qquad (5)$$

where P_g and P_{eq} are the pressure in the gas phase and in equilibrium, respectively. Equation (5) was used to calculate the hydrate formation rate constant aK^* using the experimental overall gas hydrate formation rate r_{hy}, experimental gas phase pressure P_g, and available literature data for the gas-water-hydrate equilibrium pressure P_{eq} at the experimental temperature.
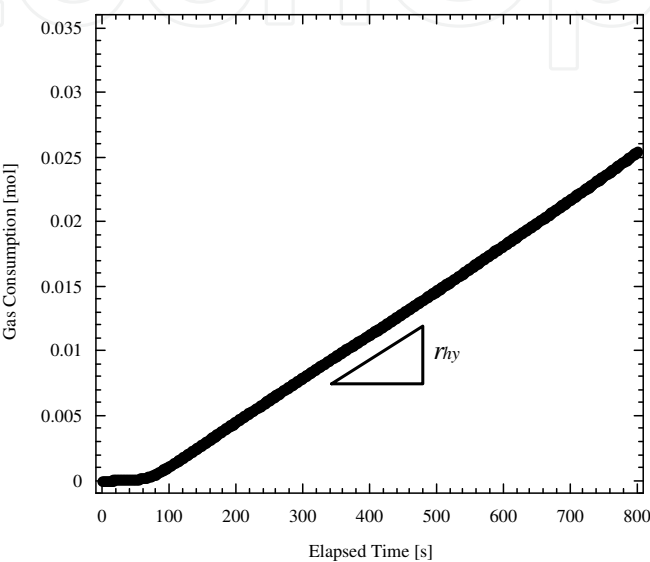
Fig. 3. Typical gas consumption line to calculate the overall hydrate formation rate (Tajima et al., 2010a).

Guest gas	aK^* [mol^2/(s·J)]	P_g [MPa]	T [K]	Reactor	Reference
CH$_2$FCF$_3$	2.08 x 10^{-8}	0.20	276.2	Author's reactor	Tajima et al., 2010a
CHClF$_2$	4.40 x 10^{-8}	0.16	276.1	Author's reactor	Tajima et al., 2011a
Xe	1.2 x 10^{-8}	3.5	275	Stirred tank	Daimaru et al., 2007
CH$_4$	6.22 x 10^{-10}	6.0	275.15	Stirred tank	Daimaru et al., 2007
CO$_2$	1.33 x 10^{-7}	6.0	277.65	Stirred tank	Li et al., 2009
SF$_6$	4.26 x 10^{-9}	0.30	276.1	Author's reactor	Tajima et al., 2011b

Table 1. A type of gas hydrate formation rate constant of various guest gases.

Figure 3 shows typical gas consumption line in the semi-batch flow reactor. During the early stage of hydrate formation, the gas consumption is very small and unequable, which is parhaps because of the hydrate nucleation and unsteady state. The gas consumption becomes constant over time because the hydrate formation in the reactor reaches a steady state. Therefore, the overall hydrate formation rate can be calculated from the slope of the gas consumption line in the late stage. For instance, Table 1 summarizes the hydrate

formation rate constant from our studies and previous literatures in which hydrate formation rate is analysed with the similar equation. In the study using the stirred tank reactor, the hydrate formation rate constant have been calculated assuming that the gas-water sytem is sufficiently agitated, that is, $k_L >> k_f$. This assumption will be discussed later. The hydrate formation rate constant aK^* for freon gas hydrate (CH_2FCF_3, $CHClF_2$) are same order of magnitude as xenon hydrate, and two order of magnitude higher than that of CH_4 hydrate. The aK^* for SF_6 hydrate was one order of magnitude lower than above freon gas hydrate. The aK^* for CO_2 hydrate is highest among above other gas hydrates. It is guessed that the gas hydrate formation rate constant may be depending on the guest gas solubility in water, but further information and investigation are necessary to confirm this relationship.

4. Relation between hydrate formation and operation conditions

This section focuses on the relation between the gas hydrate formation and the operation conditions in the semi-batch flow reactor. The overall gas hydrate formation process is very affected by varying thermodynamic, mechanical, and chemical conditions. Thermodynamic conditions are operation pressure and temperature. The gas and water flow rate are defined as the mechanical conditions because the flow rates will vary the gas-water mixing state by mixing element in the semi-batch flow reactor. Here, it is regarded as the chemical conditions that the hydrate formation promoter is added in water phase, because the additives will vary the chemical potential of water phase and interfacial tension.

4.1 Thermodynamic conditions

In general, gas hydrate formation rate constant in stirred tank and agitation is analyzed assuming that $k_L >> k_f$, but this assumption requires careful attention. In the static mixing reactor, depending on the pressure and temperature conditions (thermodynamic conditions), a single non-hydrate and main two types of hydrate formation patterns are observed regardless of target gas species. Fig.4 shows typical gas hydrate formation patterns observed in the semi-batch flow reactor. In this case, the operation temperature is gradually decreased under constant pressure or P_g increases under constant T, constant gas and water flow rates. There is a gas-water system under outside pressure and temperature conditions of hydrate equilibrium curve (Fig.4a). Under near-equilibrium conditions, the hydrate formation is not occurred (Fig.4b). The non-hydrate formation condition is probably a meta-stable region. The two types of gas hydrate formation patterns, which are detailed below, are labelled "hydrate plug" (Fig.4d) and "hydrate slurry" (Fig.4c). The hydrate plug has a target gas hydrate "shell" formed on the surface of the bubbles. Whereas the hydrate slurry consists of very small target gas hydrate particles in water and a hydrate shell rarely formed on the bubble surface (Tajima et al., 2007). The observation results imply that the formed hydrate peels and sheds from the bubble surface. Three step mechanisms of hydrate film growth at gas-water interface have been reported (Sloan & Koh, 2008); (1) thin porous hydrate film formation, (2) thick porous hydrate film formation, and (3) nonporous hydrate film formation. Hydrate slurry pattern is perhaps formed by peering and shedding porous hydrate film at Steps 1 and 2. If nonporous hydrate formation is achieved due to higher hydrate growth rate, it is difficult to shed the film and hydrate plug formation will become dominant. Hydrate slurry turned into hydrate plug with an increase in operation pressure and a decrease in

operation temperature, which means the increase in the hydrate formation rate by increasing the driving force. Therefore, the assumption, $k_L \gg k_f$, may be unsuitable depending on the hydrate formation patterns, and the hydrate shedding will be an important consideration for gas hydrate formation from gas-water system.
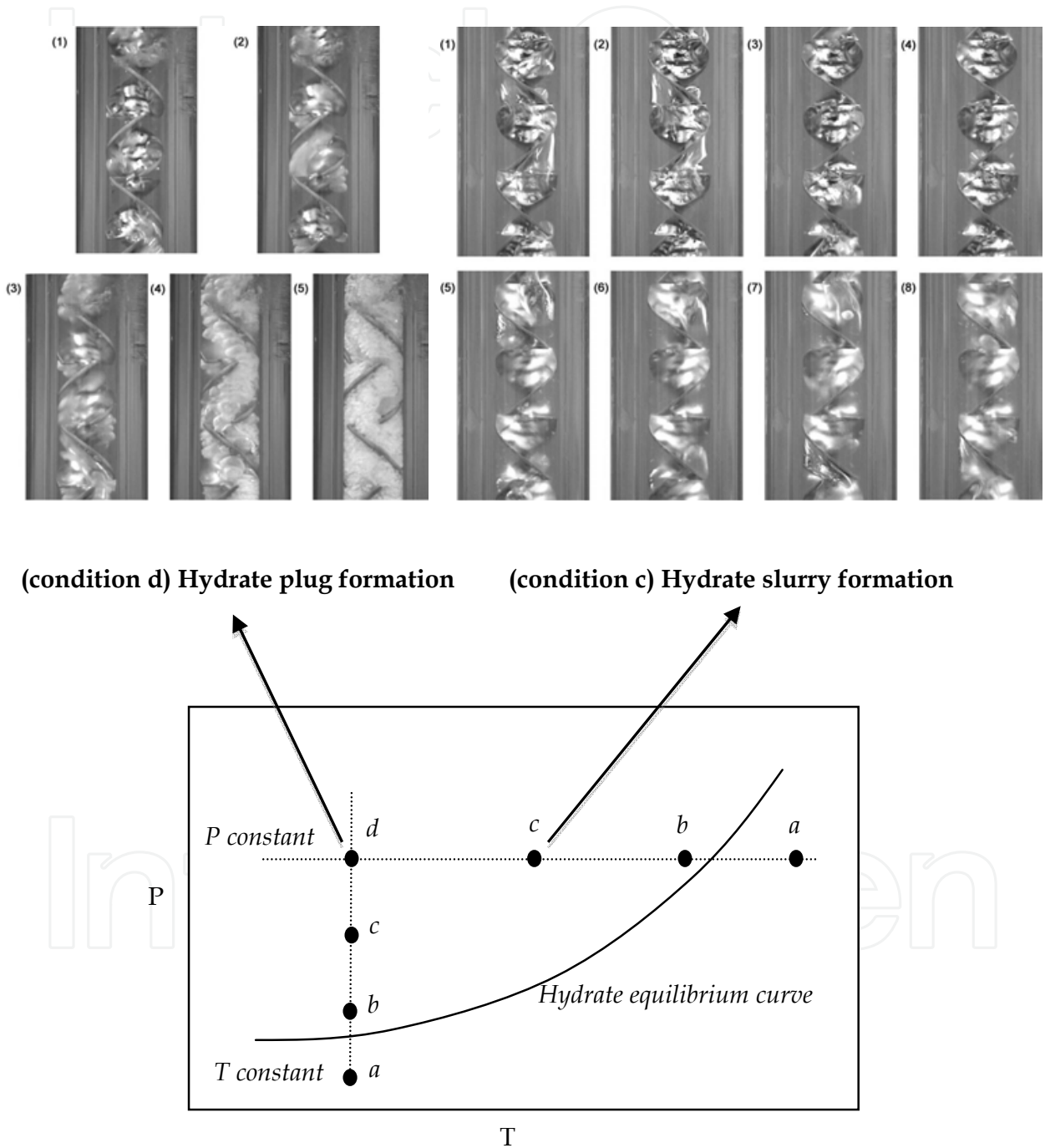

(condition d) Hydrate plug formation   **(condition c) Hydrate slurry formation**

Fig. 4. Typical gas hydrate formation patterns in the semi-batch flow reactor. Conditions (*a*) and (*b*) are gas-water system, (*c*) and (*d*) are time-course in the hydrate formation, hydrate slurry and hydrate plug (Tajima et al., 2007)

(a) operation pressure effect   (b) operation temperature effect
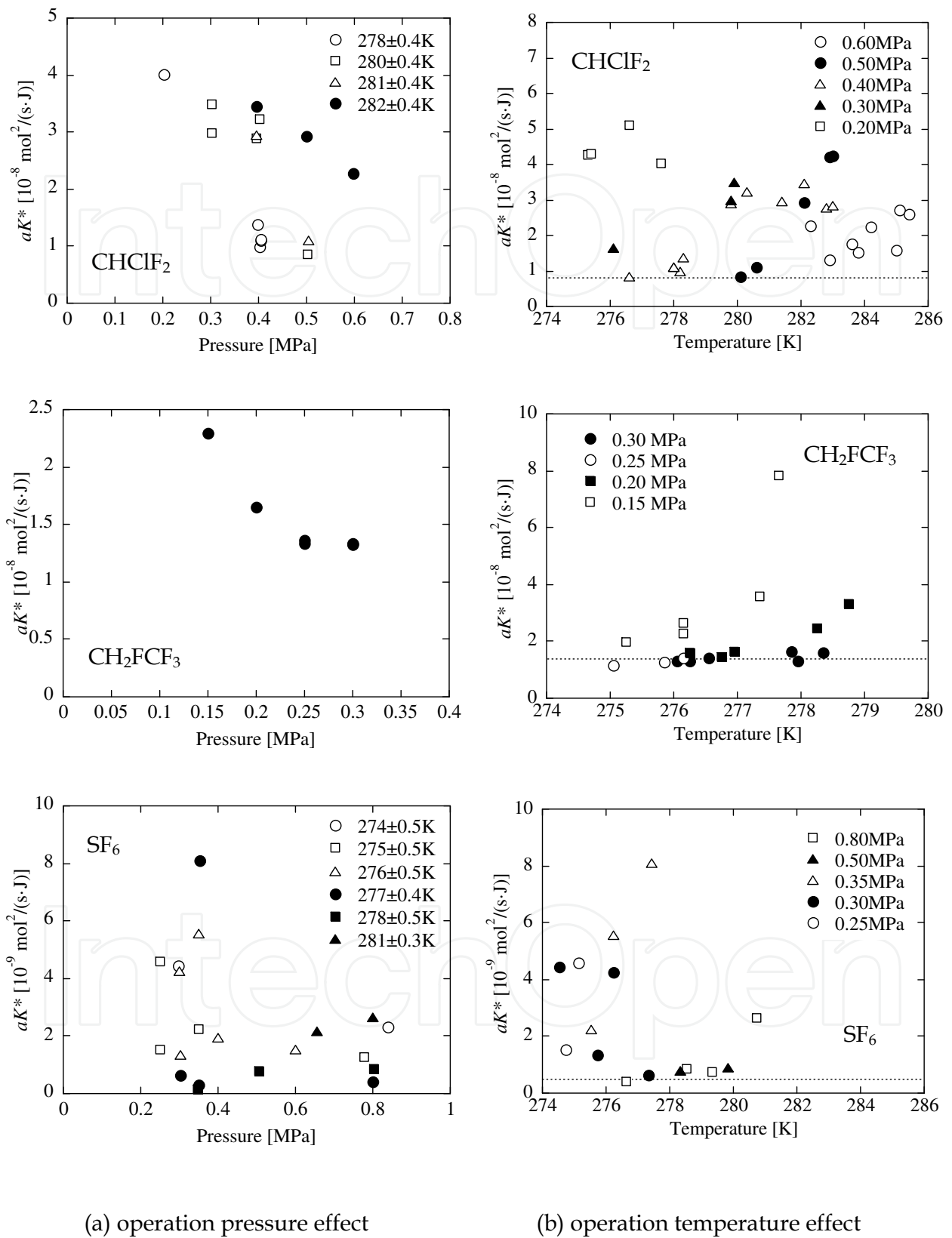
Fig. 5. Effect of operation pressure and temperature on the aK^* value of various gas hydrate at constant another one (Tajima et al., 2010a, 2011b).

Fig.5 shows the effect of operation pressure on the aK^* value of various hydrates at constant temperature. Without respect to gas species the aK^* is decreased with an increase in the operation pressure but the data for SF_6 are scattered because of very small value. Although the hydrate formation rate may increase with operation pressure increase essentially, higher formation rate leads to form the strong hydrate shell on bubble surface. The formation of strong hydrate shell on bubble surface will prevent further hydrate formation, and thus reduce the aK^*. Fig.5 also shows the effect of operation temperature on the aK^* at constant operation pressure. These conditions are corresponding to the equilibrium pressure change. The aK^* value decreases and approaches a certain value with decreasing operation temperature at constant pressure. As well as operation pressure effect, hydrate shell formation will prevent further hydrate formation.

All present gas hydrate formation shows similar trend for thermodynamic condition change; the gas hydrate formation rate constant aK^* is decreased with the increase in operation pressure and decrease in temperature. These results indicate that the hydrate formation (nucleation and crystal growth) and mass transfer are largely inhibited by the formation of strong hydrate shell at bubble surface. The gas hydrate shell is easy to form on target gas bubble when no-mixing condition. Although the static mixing operation in the reactor can accelerate the hydrate shedding and thus keep the gas-water interfacial area (Tajima et al., 2005, 2010a), higher hydrate growth rate do not allow the strong hydrate shell to shed from bubble surface. The strong hydrate shell formation implies that the hydrate crystal growth rate is higher than the mass transfer rate (which includes the shedding rate of hydrate formed at the bubble surface). Therefore, in the higher pressure and lower temperature case, hydrate formation rate constant is apparently decreased. This trend is independent with hydrate structure, sI and sII (pure $CHClF_2$ gas forms sI hydrate, and pure CH_2FCF_3 and SF_6 gas are sII hydrate).

As presented above, this hydrate shell formation inhibits hydrate growth and is decreased the aK^* value because of two causal factors mainly; decrease in the interfacial area a, and resistance to mass transfer from gas to water phase k_L. Therefore, the peel of hydrate shell from bubble surface is a point well taken for a feasible hydrate formation mechanism.

4.2 Mechanical conditions

As discussed above, for gas hydrate formation, it is necessary to prevent hydrate growth inhibition by hydrate shell formation at the bubble surface. The author investigated varying both the flow rate and direction of water flow compared with gas flow in the reactor (Tajima et al., 2010a). When changing the mechanical condition, that is the change of water-flow rate like as gas adsorption equipment, water recycling in the hydrate reactor accelerates hydrate formation. With gas-water co-current flow, the interfacial area and mixing effect of the static mixer are expected to increase, although the residence time of bubbles in the reactor decreases because they rise faster with the water flow. In contrast, a counter-flow increases the residence time. The counter-flow will also result in easier peeling and shedding of the formed hydrate from the bubble surface because of an increase in the shear force on the gas-water interface. Both water flow directions can increase the hydrate formation rate.

Fig.6 shows the effect of water-flow rate (Q_L) on freon gas ($CHClF_2$ and CH_2FCF_3) hydrate formation rate constant. A positive water flow rate indicates co-current flow to the target gas, and a negative flow rate indicates counter flow. In the complete semi-batch system, the water flow rate is zero. The vertical axis is the ratio of aK^* to one at $Q_L = 0$. Despite holding

thermodynamic conditions (operation pressure and temperature) constant for each gas, the gas hydrate formation is accelerated. Hydrate slurry formation is observed for both water flow conditions even though the hydrate shell formation is observed at $Q_L = 0$. Without respect to gas species and hydrate structure, the water flow can avoid the hydrate shell formation. In the thermodynamic condition in which the hydrate slurry is formed at $Q_L = 0$ (0.15MPa for CH_2FCF_3), the aK^* value has low dependence on water flow rate. These results indicate that under mechanical mixing condition there are two important factors in acceleration of hydrate formation; the increase in the gas-water interfacial area from breaking up bubbles and a renewal of the gas-water interface. The increase in the gas-water interface occurs with breaking up the bubble covered with hydrate shell during water-gas cocurrent flow, and causes of the continued presence of a fresh interface in the counter flow by peeling hydrate formed on bubble surface. Under thermodynamic conditions formed hydrate slurry at $Q_L = 0$, the mechanical effect is low because they meet sufficient conditions (higher hydrate peeling and shedding rate than hydrate growth rate) necessary for avoidance of hydrate shell formation. The kinetic data indicates that the overall hydrate formation rate would be equal to the mass transfer rate including the rate of hydrate peeling from the gas bubble.
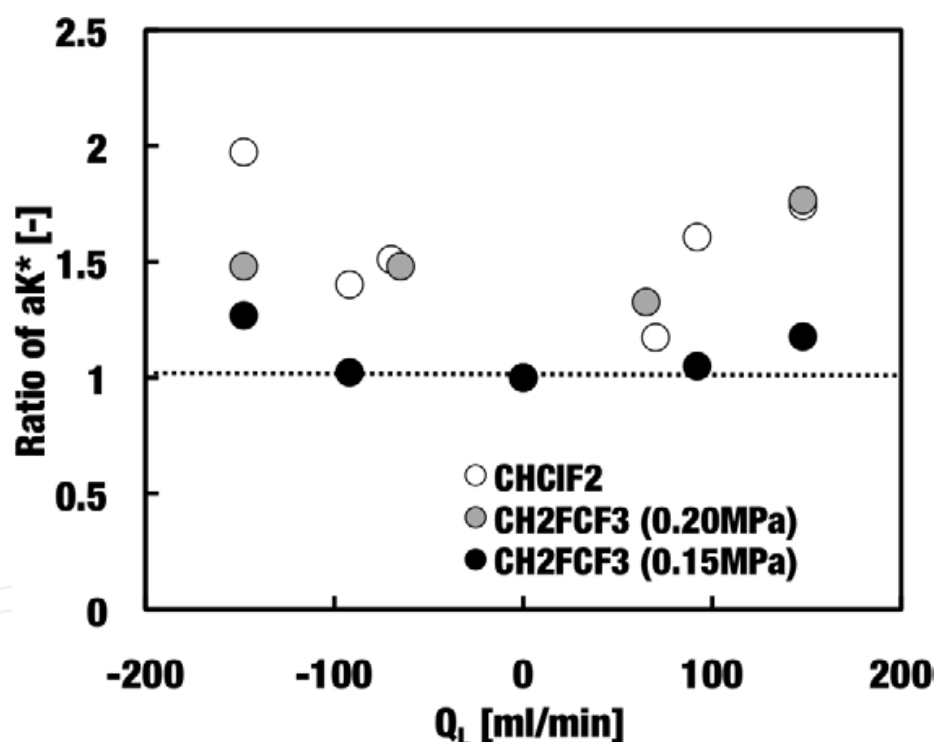

Fig. 6. Effect of water flow rate and direction on the aK^* at 275.8±0.3K for CH_2FCF_3 and 0.40MPa, 282.3±0.2K for $CHClF_2$ (Tajima et al., 2010a, 2011b).

4.3 Chemical conditions

A well-known promoter of gas hydrate is a surfactant, such as sodium dodecyl sulfate (SDS), of which the acceleration effect of the hydrate formation (Zhong & Rogers, 2000). Such surfactant additives, in the first place, have been used and investigated to prevent hydrate plug, namely hydrate inhibitor, in pipelines under certain pressure and temperature conditions because hydrate is a problem to the oil and gas industry (Huo et al., 2001). Effects

of surfactant such as SDS on gas hydrate formation have been widely investigated by many researchers, and the author has also investigated the ability of SDS to accelerate hydrate formation (Tajima et al., 2010b). Here focuses on the effect of SDS addition on the hydrate formation process under the SDS concentration below the critical micelle concentration (CMC). The surfactant additives do not shift the hydrate equilibrium condition and do not change hydrate structure, but these change the solution properties. Here the surfactant addition is defined as chemical condition for hydrate formation.

Fig.7 shows direct observation result of hydrate formation in SDS solution. From direct observation of hydrate formation, the hydrate shell is formed at the surface of bubbles in any SDS concentration, but the appearance of the hydrate shell and its behaviour are significantly changed with increasing the SDS concentration. Under the certain pressure and temperature conditions, $CHClF_2$ hydrate plug including bubble covered with the strong hydrate shell is formed (Fig.7a). Without SDS, smooth and homogenous hydrate film is formed at the surface of bubbles. Target gas is trapped in the rigid hydrate shell, and the bubbles are agglomerated each other to form a grape-like structure. Adding a small amount of SDS in water, hydrate shell formed is easily disappeared (Fig.7b). By the addition of SDS, the hydrate shell forms with rougher and heterogeneous surface; the hydrate shell seems to become loosely, and easily collapsed by the buoyant motion of target gas trapped in the shell.
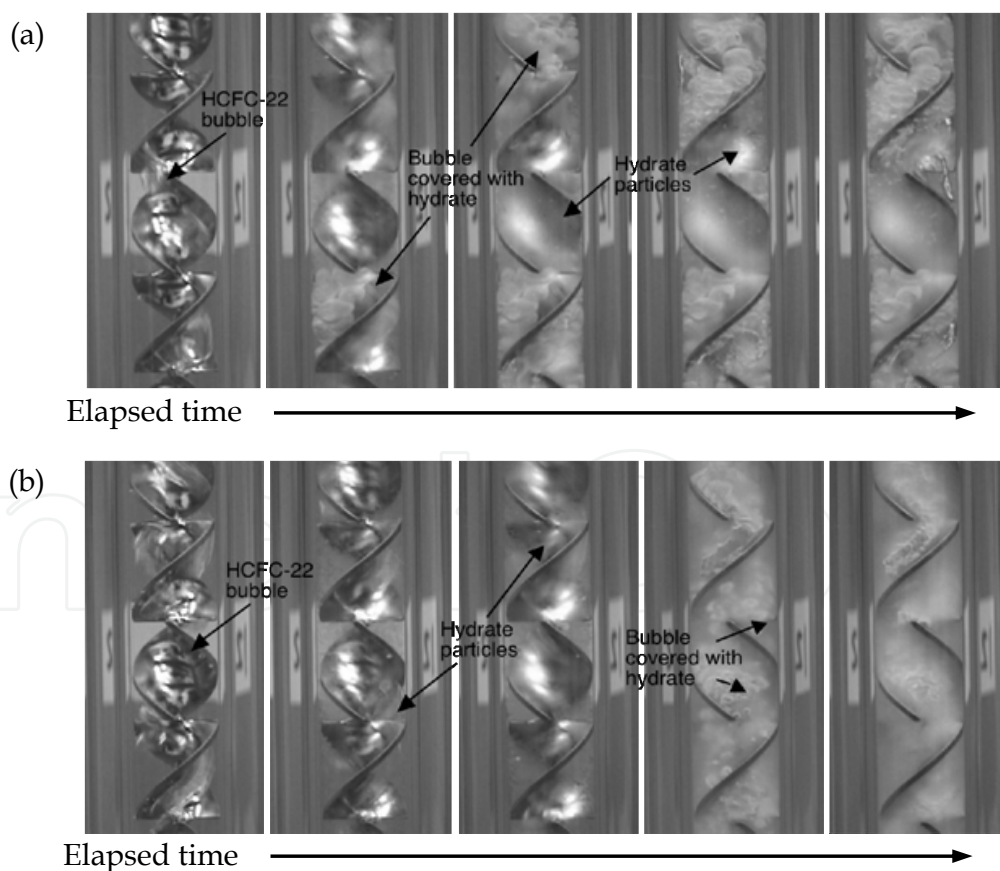
(a)

Elapsed time ⟶

(b)

Elapsed time ⟶

Fig. 7. $CHClF_2$ hydrate formation in water (a) and 400ppm SDS aqueous solution (b) at 0.40MPa, 283K (Tajima et al., 2010b).
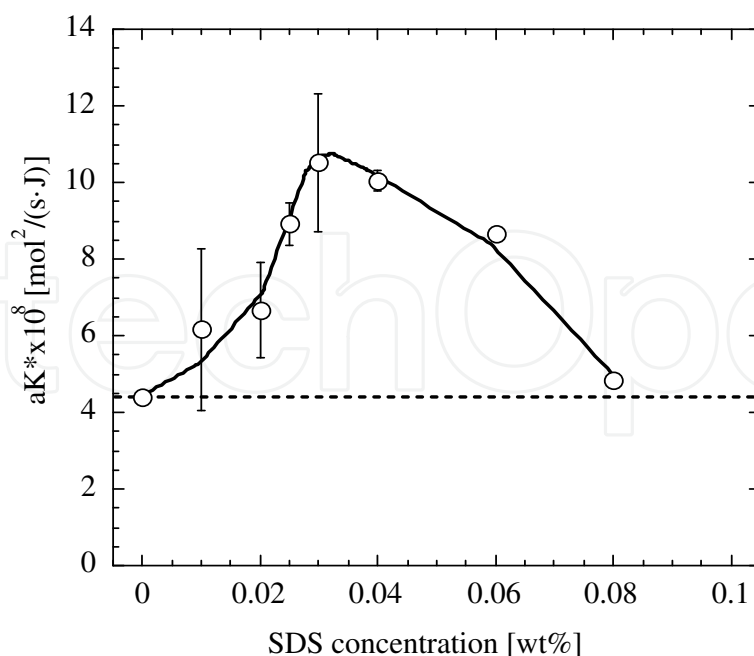
Fig. 8. Effect of SDS concentration on $CHClF_2$ hydrate formation rate constant. (Tajima et al., 2011a)

From point of view of hydrate formation kinetics, the promoting effect and the inhibition effect on gas hydrate formation emerged in each SDS concentration below CMC. Fig.8 shows the effect of SDS concentration on $CHClF_2$ hydrate formation rate constant. The value of aK^* is increased up to 0.03wt% SDS solution. The aK^* value at 0.03wt% SDS solution is 10.5×10^{-8} $mol^2/(s \cdot J)$, which is about 2.4 times larger than that in water (0wt% SDS). The aK^* value is gradually decreased as SDS concentration further increased. At 0.08wt% of SDS concentration, the aK^* value returns nearly to the level in water. There results have a similar trend to the experimental results using sodium alkylsulfonates (Daimaru et al., 2007) as promoting additive.

One of factors for promoting effect is the interfacial area, a, expansion came from the interfacial tension reduction. SDS addition in water is decreased in the surface tension of water, and thus gas bubble size before hydrate formation reduces with increasing additive concentration. In addition, SDS adsorption on bubble and hydrate surface would accelerate forming rough hydrate and peeling easily hydrate formed, that is, the increase in the overall kinetic constant, K^*. The SDS concentration range shown the promoting effect is close to that of the mono- and multi-layer adsorption of SDS on hydrate surface but the different guest molecule species (Zhang et al., 2008; Lo et al., 2008). SDS as a surfactant will promote not only the crystal growth but also the gas-liquid contact, mass transfer, with adsorption. Thus, the enhancement of the gas hydrate formation by the SDS addition can be attributed to the increase of both a and K^*.

Despite the a value is increased with increasing SDS concentration, the aK^* value is decreased with increase in SDS concentration, and furthermore, returns to the level in water. The aK^* value reduction implies that the decrease in the overall kinetic constant K^* counteracts the effect of the interfacial area expansion, which corresponds to inhibition of mass transfer or crystal growth. Although SDS cannot form own hydrate, the inhibition effect of SDS as anionic surfactant will come from their adsorption on bubbles and hydrate

particles. The previous researchers (Daimau et al., 2007) explained that the inhibition effect of the anionic surfactant is due to cover the gas-water interface with surfactant molecules. Recent research reported by zeta potential measurement that SDS adsorbs hydrate particle surface strongly and the SDS adsorption amount increases with increase in the SDS concentration (Zhang et al., 2008; Lo et al., 2008). Although zeta potential measurement for $CHClF_2$ hydrate in SDS solution cannot be carried out, the similar SDS adsorption will occur on $CHClF_2$ hydrate surface because of SDS adsorption via hydrogen bond. The author have observed the morphological change, from smooth and homogeneous to rougher and heterogeneous, of $CHClF_2$ hydrate surface that is more noticeable for the conditions with the SDS concentration higher than about 250 ppm (equal to 0.25 wt%) (Tajima et al., 2010b). The direct observation result implies that SDS molecules will absorb bubble and hydrate surface and produce a significant change in characteristic of the hydrate formed on the bubble surface for the SDS concentration. In higher SDS concentration, therefore, heavy adsorption of SDS molecules on bubbles/hydrate particles surface rather prevents $CHClF_2$ hydrate strongly from forming and growing despite the increased interfacial area with the decease in surface tension.

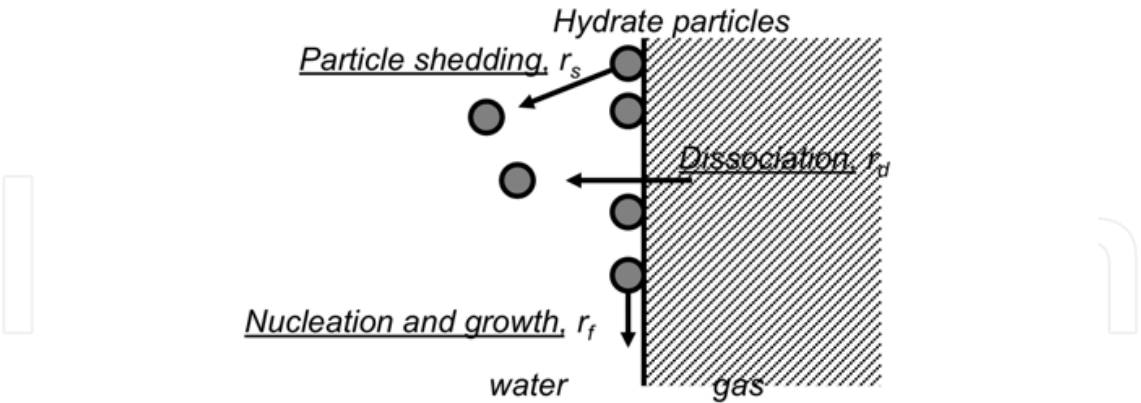## 4.4 Feasible mechanism of hydrate formation in static mixing-type flow reactor

From aforementioned above, the hydrate formation process is greatly depending on the thermodynamic, mechanical, and chemical conditions; the condition effect is appeared with the appearance of hydrate formed. The data obtained for $CHClF_2$, CH_2FCF_3, and SF_6 appears to be necessary to explain the mechanism of hydrate formation in the static mixing-type flow reactor. Here, the author can estimate a feasible hydrate formation mechanism in the static mixing type flow reactor.

The hydrate formation rate is well known to consist of crystal growth rate and dissociation rate (mass transfer rate). In addition, the author requires consideration of the hydrate shedding rate to overall hydrate formation (Tajima et al., 2005, 2010b). Therefore, the hydrate formation rate will consist mainly of the hydrate formation rate (nucleation and crystal growth that is dependant on thermodynamic conditions) and the mass transfer rate (target gas dissociation in water and target gas hydrate shedding from bubble surface that is dependant on mechanical conditions).

Fig. 9 shows the speculated mechanisms for hydrate formation in static mixing-type flow reactor according to experimental results (Tajima et al., 2004, 2005, 2011b). The r_d, r_f, and r_s are rates of target gas dissociation to water, target gas hydrate nucleation and growth, and target gas hydrate particle/film shedding, respectively. The Case A-C situations are made due to the balance among the thermodynamic, mechanical, and chemical conditions in the reactor.

Case A is for gas hydrate slurry formation. In this case, the apparent interfacial area between water and target gas phases, a, is large enough to dissociate target gas from bubble to water phase because of $r_s > r_f$. As a result, the interfacial area keeps a constant nearly and the target gas dissociation is inhibited very little by porous hydrate formation. The overall hydrate formation rate r_{hy} depends on the K^* value (that is, k_L and k_f in Eq.(2)) mainly. Because continuous hydrate particle formation can be occurred, the overall hydrate formation rate constant aK^* is high. This situation is relation to mild thermodynamic conditions (lower pressure and higher temperature), high mechanical mixing conditions (high water flow rate), and lower additive concentration.

(a) Slurry formation, Higher r_d and r_s (large apparent interface area)

(b) Intermediate (decreasing apparent interface area)
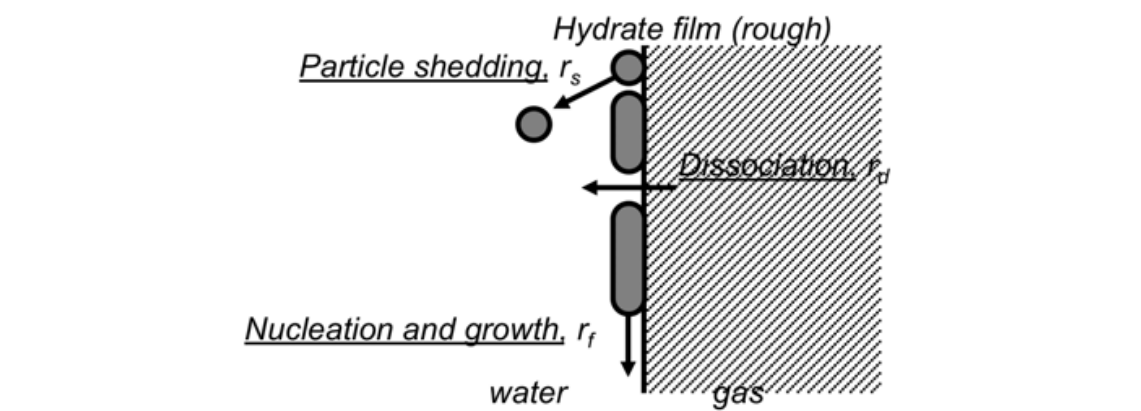
(c) Shell formation, Lower r_d and r_s (small apparent interface area)
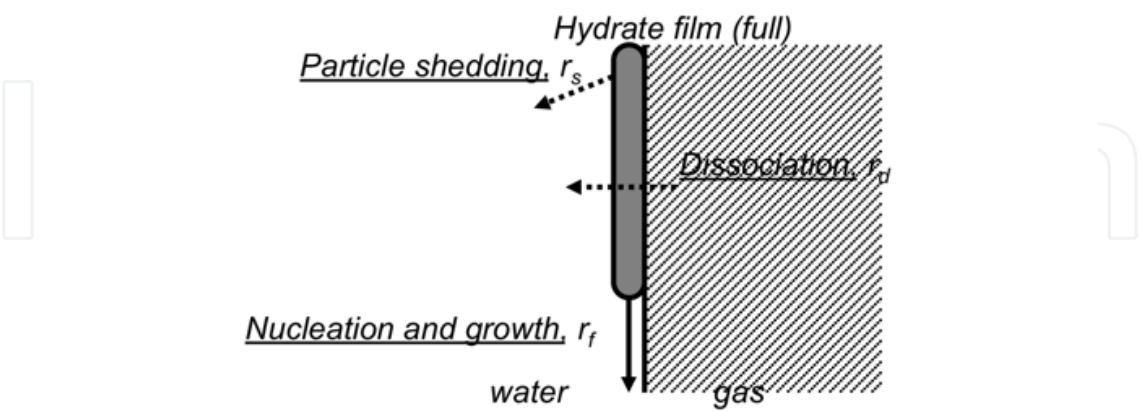

Fig. 9. Speculated mechanisms of hydrate formation in static-mixing type flow reactor (Tajima et al., 2011b)

Case C is for strong hydrate shell formation. In this case, the target gas bubbles are rapidly covered with strong hydrate shell because the hydrate formation rate r_f is relatively higher

than shedding rate r_s. The apparent interfacial area between gas and water, a, is considerably restricted and also the dissociation rate r_d is considerably decreased (for example, a similar situation have been observed in the case of CO_2 hydrate formation (Ogasawara et al., 2001)). As a result, there is little the further hydrate formation, and thus the overall hydrate formation rate constant aK^* is low depending on r_d and r_s. This hydrate formation occurs under hard thermodynamic conditions (higher pressure and lower temperature) and lower mechanical mixing conditions. Although the additive addition can prevent the strong hydrate shell, sufficient mechanical condition is necessary to form further hydrate with accelerating the hydrate shedding process.

Case B is for porous and rough hydrate particle/film formation and the intermediate case between Cases A and C. Hydrate particles and partial hydrate film are formed on bubble surface. The film pore and void channels allow target gas to diffuse into water phase (Sloan & Koh, 2008), and partial hydrate shedding is occurred on bubble surface. The apparent interfacial area between target gas and water, however, is decreased and the dissociation of target gas into water is limited by rough hydrate film formation. As a result, the aK^* value (not only a but also K^* values) is lower than that for Case A. In another case, higher concentration of additive in water phase will contribute to keep porous and rough hydrate film (Case B) with preventing hydrate growth (Tajima et al., 2010b). That is, additives (like as surfactants) adsorbing on bubble surface can keep the gas dissociation and the hydrate shedding rates.

If the solubility in water is very low, the dissociation rate (mass transfer rate) will be low. As a result, the overall formation rate is low. For example, relatively high solubility of CH_2FCF_3 and $CHClF_2$ (near CO_2 solubility in water) leads to higher dissociation rate and hydrate formation rate. On the other hand, lower solubility of SF_6 (near CH_4 solubility in water) cause lower dissociation rate. This trend is in agreement with the data obtained in this study (Table 1). The dissociation rate may be a rate-controlling step. Further investigation is necessary for hydrate formation rate equation.

5. Conclusion

The gas hydrate formation kinetics is investigated in the semi-batch flow reactor equipped with static mixer, and thus discusses the hydrate formation process based on the experimental data by varying thermodynamic, mechanical, and chemical conditions. In the flow reactor, there are multiple flows with gas-liquid-solid system, and the gas hydrate formation process is overly complicated. There are mainly two hydrate formation patterns in the reactor; hydrate slurry and hydrate plug. According to the experimental observation and results, the gas hydrate formation process consists of the hydrate nucleation, hydrate growth, hydrate shedding, and gas dissociation processes. Especially, the idea of the hydrate shedding from the interface is very important. The balance among these processes is altered under thermodynamic, mechanical, and chemical conditions. For the application of the gas hydrate technologies, it is necessary to not only convert sufficiently (mixture) gas to hydrate but also form hydrate appearance to transport and apply easy. Many researchers have investigated about the thermodynamic and chemical conditions in stirred tank, but the mechanical conditions have been less noticed. The static mixer in the flow reactor improves the mixing function in the reactor. Although it is perhaps difficult to find out the essential hydrate formation rate, the author expects that these results help the engineering application of gas hydrate.

6. Acknowledgment

7. References

Daimaru, T.; Yamasaki, A. & Yanagisawa, Y. (2007). Effect of Surfactant Carbon Chain Length on Hydrate Formation Kinetics, *Journal of Petroleum Science and Engineering*, Vol.56, No.1-3, (March 2007), pp.89-96, ISSN 0920-4105

Englezos, P.; Kalogerakisa, N.; Dholabhaia, P.D. & Bishnoi, P.R. (1987) Kinetics of Formation of Methane and Ethane Gas Hydrates, *Chemical Engineering Science*, Vol.42, No.11, (November 1987), pp.2647-2658, ISSN 0009-2509

Fukumoto, K.; Tobe, J.; Ohmura, R. & Mori, Y.H. (2001). Hydrate Formation Using Water Spraying in a Hydrophobic Gas: A Preliminary Study, *AIChE Journal*, Vol.47, No.8, (August 2001), pp.1899-1904, ISSN 0001-1541

Godfrey J. C. (1997). Static Mixer, In: *Mixing in the process industries*, Harnby, N.; Edwards, M. F.; Nienow, A. W. (Eds.), 225-249, Butterworth-Heinemann, ISBN 0-7506-3760-9, Oxford, UK.

Gudmundsson, J. S. & Børrehaug A. (1996). Frozen Hydrate for Transport of Natural Gas, *Proceedings of 2nd International Conference on Natural Gas Hydrates*, pp439-446, Toulouse, France, June2-6, 1996.

Hashemi, S.; Macchi, A. & Servio, P. (2009) Gas-Liquid Mass Transfer in a Slurry Bubble Column Operated at Gas Hydrate Forming Conditions. *Chemical Engineering Science*, Vol.64, No.19, (October 2009), pp.3709-3716, ISSN 0009-2509

Huo, Z.; Freer, E.; Lamar, M.; Sannigrahi, B. ; Knauss, D. M. & Sloan E. D. (2001). Hydrate Plug Prevention by Anti-Agglomeration, *Chemical Engineering Science*, Vol.56, No.17, (September 2001), pp.4979-4991, ISSN 0009-2509

Kang, S.-P. & Lee, H. (2000). Recovery of CO_2 from Flue Gas Hydrate: Thermodynamic Verification Through Phase Equilibrium Measurements, *Environmental Science and Technology*, Vol.34, No.20, (October 2000), pp.4397-4400, ISSN 0013-936X

Lee, H. ; Lee, J. W.; Kim, D. Y.; Park, J.; Seo, Y. T.; Zeng, H.; Moudrakovski, I. L.; Ratcliffe, C. I. & Ripmeester, J. A. (2005). Tuning Clathrate Hydrates for Hydrogen Storage, *Nature*, Vol.434, 7 April, (April 2005), pp.743-746, ISSN 0028-0836

Li, S.; Fan, S.; Wang, J.; Lang, X. & Liang, D. (2009). CO_2 Capture from Binary Mixture via Forming Hydrate with the Help of Tetra-n-Butyl Ammonium Bromide, *Journal of Natural Gas Chemistry*, Vol.18, No.1, (March 2009), pp.15-20, ISSN 1003-9953

Lo, C. ; Zhang, J.S.; Somasundaran, P.; Lu, S.; Couzis, A. & Lee, J.W. (2008). Adsorption of Surfactants on Two Different Hydrates, *Langmuir*, Vol.24, No.22, (November 2008), pp.12723-12726, ISSN 0743-7463

Luo, Y.-T.; Zhu, J.-H.; Fan, S.-S. & Chen, G.J. (2007). Study on the Kinetics of Hydrate Formation in a Bubble Column, *Chemical Engineering Science*, Vol.62, No.4, (February 2007), pp.1000-1009, ISSN 0009-2509

Nagata, T.; Tajima, H.; Yamasaki, A.; Kiyono, F. & Abe, Y. (2009). An Analysis of Gas Separation Processes of HFC-134a from Gaseous Mixtures with Nitrogen-Comparison of Two Types of Gas Separation Methods, Liquefaction and Hydrate-Based Methods, in Terms of the Equilibrium Recovery Ratio, *Separation and Purification Technology*, Vol.64, No.3, (January 2009), pp.351-356, ISSN 1383-5866

Ogasawara, K.; Yamasaki, A. & Teng, H. (2001). Mass transfer from CO_2 Drops Traveling in High-Pressure and Low-Temperature Water, *Energy & Fuels*, Vol.15, No.1, (January 2001), pp.147-150, ISSN 0887-0624

Sloan, E. D.; Koh, C. A. (2008). *Clathrate Hydrates of Natural Gases, 3rd Ed.*, CRC Press, ISBN 978-0-8493-9078-4, Boca Raton, Florida, USA.

Szymcek, P.; McCallum, S.D.; Taboada-Serrano, P. & Tsouris, C. (2008). A Pilot-Scale Continuous-Jet Hydrate Reactor, *Chemical Engineering Journal*, Vol.135, No.1-2, (January 2008), pp.71-77, ISSN 1385-8947

Tajima, H.; Yamasaki, A. & Kiyono, F. (2004). Continuous Formation of CO_2 Hydrate via a Kenics-type Static Mixer, *Energy & Fuels*, Vol.18, No.5, (September 2004), pp.1451-1456, ISSN 0887-0624

Tajima, H.; Yamasaki, A. & Kiyono, F. (2005). Effects of Mixing Functions of Static Mixers on the Formation of CO_2 Hydrate from the Two-Phase Flow of Liquid CO_2 and Water, *Energy & Fuels*, Vol.19, No.6, (November 2005), pp.2364-2370, ISSN 0887-0624

Tajima, H.; Nagata, T.; Yamasaki, A.; Kiyono, F. & Masuyama, T. (2007) Formation of HFC-134a Hydrate by Static Mixing, *Journal of Petroleum Science and Engineering*, Vol.56, No.1-3, (March 2007), pp.75-81, ISSN 0920-4105

Tajima, H.; Nagata, T.; Abe, Y.; Yamasaki, A.; Kiyono, F. & Yamagiwa, K. (2010a). HFC-134a Hydrate Formation Kinetics During Continuous Gas Hydrate Formation with a Kenics Static Mixer for Gas Separation, *Industrial and Engineering Chemistry Research*, Vol.49, No.5, (March 2010), pp.2525-2532, ISSN 0888-5885

Tajima, H.; Kiyono, F. & Yamasaki, A. (2010b). Direct Observation of the Effect of Sodium Dodecyl Sulfate (SDS) on the Gas Hydrate Formation Process in a Static Mixer, *Energy & Fuels*, Vol.24, No. 1, (January 2010), pp.432-438, ISSN 0887-0624

Tajima, H.; Oota, Y. & Yamagiwa, K. (2011a). Effects of "Promoter" on Structure I Hydrate Formation Kinetics, In: *Physics and Chemistry of Ice 2010*, Y. Furukawa, G. Sazaki, T. Uchida, N. Watanabe (Ed.), pp.253-259, Hokkaido University Press, ISBN 978-4-8329-0361-6, Sapporo, Japan.

Tajima, H.; Oota, Y.; Yoshida, H. & Yamagkiwa, K. (2001b). Experimental Study for Gas Hydrate Formation and Recovery of Fluorine-Containing Compound in Static Mixing-type Flow Reactor, *Proceedings of 7th International Conference on Gas Hydrate*, Edinburgh, Scotland,UK, July 17-22, 2011.

Warzinski, R. P.; Riestenberg, D.E.; Gabitto, J.; Haljasmaa, I.V.; Lynn, R.J. & Tsouris, C. (2008). Formation and Behavior of Composite CO_2 Hydrate Particles in a High-Pressure Water Tunnel Facility, *Chemical Engineering Science*, Vol.63, No.12, (June 2008), pp.3235-3248, ISSN 0009-2509

Zhang, J.S.; Lo, C.; Somasundaran, P.; Lu, S.; Couzis, A. & Lee, J.W. (2008). Adsorption of Sodium Dodecyl Sulfate at THF Hydrate/Liquid Interface, *Journal of Physical Chemistry C*, Vol.112, No.32, (August 2008), pp.12381-12385, ISSN 1932-7447

Zhong, Y. & Rogers, R. E. (2000). Surfactant effects on gas hydrate formation, *Chemical Engineering Science*, Vol. 55, No.19, (October 2000), pp. 4175-4187, ISSN 0009-2509
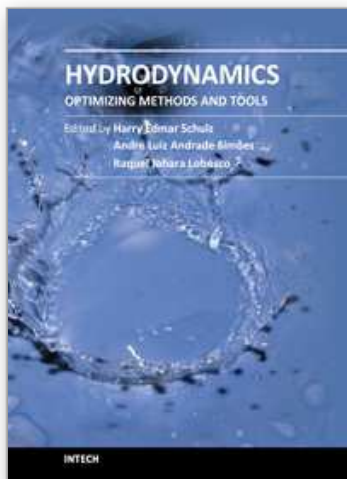
Hydrodynamics - Optimizing Methods and Tools

Edited by Prof. Harry Schulz

The constant evolution of the calculation capacity of the modern computers implies in a permanent effort to adjust the existing numerical codes, or to create new codes following new points of view, aiming to adequately simulate fluid flows and the related transport of physical properties. Additionally, the continuous improving of laboratory devices and equipment, which allow to record and measure fluid flows with a higher degree of details, induces to elaborate specific experiments, in order to shed light in unsolved aspects of the phenomena related to these flows. This volume presents conclusions about different aspects of calculated and observed flows, discussing the tools used in the analyses. It contains eighteen chapters, organized in four sections: 1) Smoothed Spheres, 2) Models and Codes in Fluid Dynamics, 3) Complex Hydraulic Engineering Applications, 4) Hydrodynamics and Heat/Mass Transfer. The chapters present results directed to the optimization of the methods and tools of Hydrodynamics.

How to reference

In order to correctly reference this scholarly work, feel free to copy and paste the following:

INTECH
open science | open minds